Geometry-based Modeling and Simulation of 3D Multipath Propagation Channel with Realistic Spatial Characteristics

Fedorov, Aleksei; Zhang, Haibo; Chen, Yawen

Published in:
2017 IEEE International Conference on Communications (ICC)

DOI:
10.1109/ICC.2017.7997381

2017

Document Version:
Peer reviewed version (aka post-print)

Geometry-based Modeling and Simulation of 3D Multipath Propagation Channel with Realistic Spatial Characteristics

Aleksei Fedorov, Haibo Zhang, and Yawen Chen
Department of Computer Science, University of Otago, Dunedin, New Zealand,
Emails: {aleksei, haibo, yawen}@cs.otago.ac.nz

***Abstract*—For high-resolution massive MIMO and very large antenna arrays, wireless channel models have to scrutinize the detailed space features of the surrounding environment. Existing models such as WINNER and 3GPP are not appropriate for validating and evaluating new concepts for 4G/5G as they do not consider the spatial characteristics of the real environment. Several geometry-based channel models have been proposed by exploiting ray tracing and considering simplified 3D shapes of buildings and objects modeled using only vertical and horizontal planes. However, the channel in these models may significantly differ from the real channel due to the inaccuracy of the object shapes. In this paper, we present an approach to model the specular reflection of a signal from an arbitrary inclined surface as well as the change of signal polarizations. We further use this approach to simulate MIMO antennas. The proposed scheme was validated through simulating LTE uplink transmissions in a real environment modeled based on Google Maps. Results showed the importance of considering detailed 3D characteristics of the surroundings in simulations. We observed that even slightly inclined walls can have significant influence on channels in comparison with models with only vertical and horizontal surfaces due to different propagation paths, different angles of reflection, and different changes of polarizations.**

I. Introduction

The wireless signal propagation environment is very complex in terms of accurate modeling. It is a challenging task to take into account all factors such as shapes of landscapes, buildings, moving objects, trees/foliage etc. Even though field experiments are more appropriate for validating new concepts and approaches on wireless communication than simulation tests, field tests are commonly very expensive and time-consuming. Hence, new concepts in wireless communication are generally first validated through simulation, which demands the simulation models to be realistic enough to provide all required effects of a real propagation environment.

In the wireless communication field, the multipath propagation channel is widely used to model the wireless signal propagation environment. It exploits the ray tracing approach and takes into account physical conditions where a transmitted signal undergoes reflections, diffractions and scattering from different obstacles [1]. While the multipath signal propagation enables communication when the Line-of-Sight (LoS) direction is blocked, it also has other effects including destructive and constructive interference and phase shifting of the signal. Such destructive effects can have harmful impacts on the power of the received signal and make the signal undecodable due to low Signal to Noise Ratio (SNR). Hence, it is vital to develop a simulation module that could model such effects, which in turn allows the development of efficient solutions to deal with the effects.

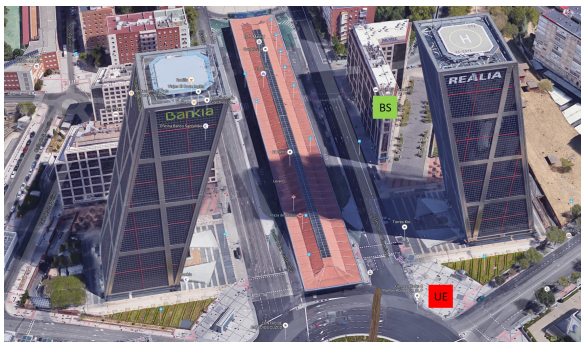

Fig. 1. The Gate of Europe in Madrid of Spain are twin inclined office buildings. If we have the base station (BS) and user equipment (UE) deployed as shown in the figure, the signals between these two devices can be reflected by the twin office buildings.

Existing 3-Dimensional multipath models can be generally divided into three groups: Stochastic Channel (SC) models [2] [3] [4], Geometry-based Channel (GC) models [5][6], and the combination of the above two [7]. The SC models have comparatively low complexity, but do not consider specific environment features, whereas a local medium is the main determining factor of a channel. Therefore, SC models are not suitable to validate new concepts such as beamforming and radio resource reuse that require specific characteristics of a local environment to deal with spatial properties of a channel. On the other hand, the GC models consider the impact of surrounding infrastructures, but they consider only simple shapes of objects described using vertical and horizontal planes. Meanwhile, many objects in a real environment have complex shapes with inclined surfaces (e.g. Fig 1) that can have a significant impact on channel behavior. Consequently, the modeled channel may significantly differ from the real channel due to the inaccuracy of object shapes representations. In addition, the recent METIS project [7] shows that existing models are inadequate for 5G requirements. These facts motivated us to investigate new realistic models.

The goal of this paper is to examine the significance of inclined surfaces in the simulation of a radio channel. The

obvious way to help us achieve this goal is to compare the channels generated by an environment with inclined walls and an environment with vertical walls. To explain the difference between the channels, consider the example shown in Fig. 2. The Base Station (BS) receives two copies of the signal from the User Equipment (UE): one comes through LoS, and the other is reflected from the wall. Assume that the wavelength of the signal is $\lambda = 12$ cm (the frequency of the carrier is $F_c = 2.6$ GHz, which is typical for LTE systems). If the lengths of the paths differ about 6 cm or $6 + 12 \cdot k$ cm where $k \in \mathbb{Z}$, the two copies in superposition give a strongly attenuated signal, i.e. the Deep Fading (DF) effect. This example shows that even a small displacement of the wall within 12 cm can totally change the channel. In the same way, the inclination of the wall can affect the channel due to changes of the propagation as the illustrated dashed lines in Fig. 2. Hence, the accurate representation of an environment is crucial for channel simulation.

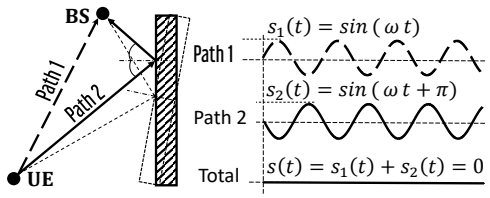

Fig. 2. The effect of DF when the reflected copies of the signal in superposition give a strongly attenuated signal regardless the power of the transmitted signal. The inclination of the wall changes the reflected path.

Fortunately, the recent Geographical Information Systems (GIS) together with Photogrammetry [8] can provide very accurate geometric models of surroundings. Thus, it is worth to incorporate accurate GIS models into a simulation of a multipath propagation channel. The resulting channel models will have all required spatial properties and will be suitable to test new concepts including the forecasting of the optimal BS positions, which has a big demand in the network planning applications.

In this paper, we present an approach to model the reflection of signals from an arbitrary inclined surface by taking into account the polarization of signals. We incorporated Google Maps data into the simulation model and validated the necessity to consider inclined walls. The simulations show a significant difference between the channel with inclined walls and the channel with vertical walls. Finally, we implemented both spherical and plane propagation waves and found that the difference between two waves is small for small antenna arrays and is significant for big antenna arrays.

The rest part of this paper is structured as follows: Section II discusses the related work. The approach to model reflection from an arbitrary inclined surface and polarization change is described in Section III. The simulation of MIMO antenna is presented in Section IV; Sections V discusses the simulation results, and the paper is concluded in Section VI.

II. Related work

The 3D SC models such as WINNER [3] and 3GPP [4] were popular because they have reasonable complexity and meet the requirements of the previous communication systems such as 2G and 3G. The major drawback is that they do not deal with geometric locations of scattering clusters but exploit the measured statistics to choose the multipath parameters such as angles of arrival and departure, propagation delays, and coefficients of power attenuation. A comprehensive extension of WINNER is the Quadriga model [2], which is a full 3D cluster-based quasi-deterministic model with the option to simulate polarization of signals. The deterministic part covers the modeling of moving UEs, and the stochastic part is mostly based on the WINNER channel model. However, in the case of channel evolution, the orientation of a cluster does not change appropriately regarding the movements of UE. For instance, the Angle of Departure (AoD) for a moving UE is remaining unchanged, while the Angle of Arrival (AoA) is changing. This causes spatial inconsistency, which is a general problem for all existing SC models.

The channels in GC models become more spatially consistent, but only exploit vertical and horizontal planes to simulate propagation effects. GEMV2 [5] simulates a channel based on information about vehicles, buildings and foliage outlines, which is taken from OpenStreetMap and traffic video records. To avoid simulation complexity, GEMV2 works with a small area with round-trip-distance less than 500 meters. Although the simulation results are consistent with the measurements, the calculation of reflections is based on 2D map, which is fair for a flat area but not for a hilly area.

The recent project METIS [7] gives a list of requirements regarding modeling of a wireless channel including accurate 3D modeling of surroundings, antenna polarization, and the spread of spherical waves, and proposes a new wireless model with the aim to improve the spatial consistency of channel model. By experimentally measuring many signal propagation effects and comparing with simulation results, it is observed that the existing models are inadequate for 5G requirements and cannot cover the required scenarios and environmental influences. The main drawback of the METIS model is that it is strictly limited by consideration of vertical walls, instead of inclined walls, to simulate the major interaction effects of signals with obstacles such as specular reflection and changes of polarization. Meanwhile, polarization is very sensitive to the parameter of inclination because the parallel and perpendicular components of polarization have different coefficients of reflection. Hence, if the physical properties of materials are known, then the channel model has to scrutinize the inclination of walls to make the model more realistic and accurate.

III. Specular reflection of a signal from an arbitrary inclined surface

In this section, we model the specular reflection of a signal from an arbitrary inclined surface. For the sake of simplicity, we start the description from the consideration of a smooth surface and then extend it to a rough surface. We assume

that all reflections are modeled according to the Law of Reflection and the ray tracing approach, i.e. the angle between the incident ray and the normal vector of the reflection surface is equal to the angle between the reflected ray and the normal vector, and the reflection proceeds in the plane perpendicular to the reflection surface. Also, we do not consider reflections with two or more bounces because, in most practical cases, the energy of a transmitted signal sharply drops after the second reflection according to the Fresnel coefficients of reflection [9]. We explain our modeling using Uplink signals (from UE to BS) because the reflections of Uplink and Downlink signals can be modeled similarly.

A. Reflection from an arbitrary plane

As illustrated in Fig. 3, plane S_1 is the reflection plane, plane S_2 is perpendicular to S_1, and point K is the reflection point. Suppose UE is a transmitter and BS is a receiver with coordinates $\mathbf{UE}$ and $\mathbf{BS}$, respectively.

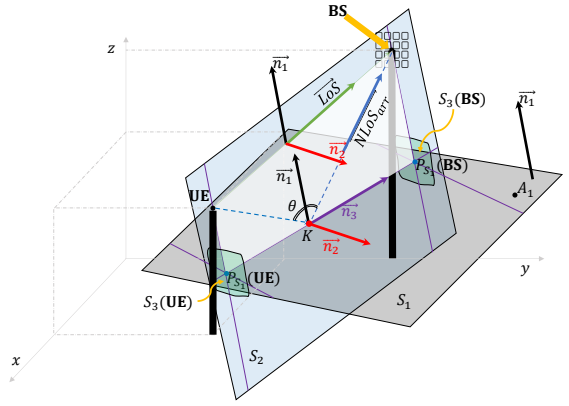

Fig. 3. Illustration of the Law of Refection.

Each plane can be defined by its normal vector and a point, through which the plane goes. In the remaining sections of this paper, all normal vectors are assumed to be unit vectors. Suppose plane S_1 has the normal vector $\vec{n}_1 = (n_{11}, n_{12}, n_{13})$ and a point $A_1 = (x_1, y_1, z_1)$. Hence, it can be represented as follows:

$$\vec{n}_1 \cdot (x, y, z) - \vec{n}_1 \cdot A_1 = 0. \tag{1}$$

Here, the notation " $\cdot$ " means the dot product.

As shown in Fig. 3, the vector of Line-of-Sight can be defined by:

$$\overrightarrow{LoS} = \frac{\mathbf{BS} - \mathbf{UE}}{d_{LoS}}, \tag{2}$$

where $d_{LoS} = \|\mathbf{BS} - \mathbf{UE}\|$ is the Euclidan distance between UE and BS. Since S_1 and S_2 are perpendicular to each other and the points $\mathbf{UE}, \mathbf{BS}$ and K are on S_2, the normal vector $\vec{n}_2$ of the plane S_2 is the cross product of $\overrightarrow{LoS}$ and $\vec{n}_1$, that is, $\vec{n}_2 = \frac{\overrightarrow{LoS} \times \vec{n}_1}{\left\|\overrightarrow{LoS} \times \vec{n}_1\right\|}$, and plane S_2 can be defined as follows:

$$\vec{n}_2 \cdot (x, y, z) - \vec{n}_2 \cdot \mathbf{UE} = 0. \tag{3}$$

To define the path/trajectory of the reflected signal inside S_2, we first find the intersection of planes S_1 and S_2, which is a line with the direction vector $\vec{n}_3 = \vec{n}_1 \times \vec{n}_2$, and then find the reflection point K. We construct two planes $S_3(\mathbf{UE})$ and $S_3(\mathbf{BS})$ that are perpendicular to both S_1 and S_2 as follows:

$$\vec{n}_3 \cdot (x, y, z) - \vec{n}_3 \cdot \mathbf{UE} = 0, \ \vec{n}_3 \cdot (x, y, z) - \vec{n}_3 \cdot \mathbf{BS} = 0.$$

As illustrated in Fig. 3, the projections $P_{S_1}(\mathbf{UE})$ and $P_{S_1}(\mathbf{BS})$ of points $\mathbf{UE}$ and $\mathbf{BS}$ on S_1 can be found as intersections of planes $\{S_1, S_2, S_3(\mathbf{UE})\}$ and $\{S_1, S_2, S_3(\mathbf{BS})\}$, respectively.

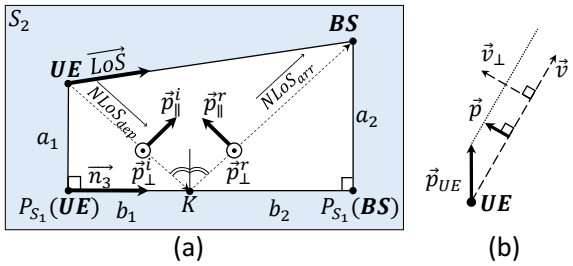

Fig. 4. (a) Reflection of the signal inside the plane S_2. (b) Polarization changes according to the observed direction.

Once $P_{S_1}(\mathbf{UE})$ and $P_{S_1}(\mathbf{BS})$ are defined, we can find the point K as illustrated in Fig. 4(a). The point K divides the segment $[P_{S_1}(\mathbf{UE}), P_{S_1}(\mathbf{BS})]$ with length $d = \|P_{S_1}(\mathbf{UE}) - P_{S_1}(\mathbf{BS})\|$ into two segments with lengths b_1 and b_2. The segments $[\mathbf{UE}, P_{S_1}(\mathbf{UE})]$ and $[\mathbf{BS}, P_{S_1}(\mathbf{BS})]$ have lengths $a_1 = \|\mathbf{UE} - P_{S_1}(\mathbf{UE})\|$ and $a_2 = \|\mathbf{BS} - P_{S_1}(\mathbf{BS})\|$, respectively. According to the Law of Reflection, $\measuredangle P_{S_1}(\mathbf{UE}) K \mathbf{UE} = \measuredangle P_{S_1}(\mathbf{BS}) K \mathbf{BS}$. Hence, we have

$$b_1 = \frac{a_1 \cdot d}{a_1 + a_2}, \ b_2 = \frac{a_2 \cdot d}{a_1 + a_2}.$$

Finally, the coordinates of the point K can be found as

$$K = P_{S_1}(\mathbf{UE}) + b_1 \cdot \vec{n}_3.$$

The exact trajectory of the reflected signal inside S_2 is defined through the arrival and departure directions, which are called as Non-Line-of-Sight (NLoS) arrival and departure, and can be computed as follows:

$$\overrightarrow{NLoS_{arr}} = \frac{\mathbf{BS} - K}{\|\mathbf{BS} - K\|}, \quad \overrightarrow{NLoS_{dep}} = \frac{K - \mathbf{UE}}{\|K - \mathbf{UE}\|}. \tag{4}$$

As shown in Fig. 4(a), the total distance covered by the reflected signal is:

$$d_{NLoS} = \|\mathbf{BS} - K\| + \|K - \mathbf{UE}\|. \tag{5}$$

B. Perpendicular and parallel components of polarization

The polarization of a signal is defined by the direction of its electric field, which is perpendicular to the direction of signal propagation [10]. However, a signal is transmitted from an antenna, and consequently the antenna defines the polarization of a signal. The polarization of antenna is a quite complex concept in terms of physics. Very roughly, the polarization of an antenna can be defined by the direction of its transducer element, which converts electric current to electromagnetic waves

and vice-versa. We define polarizations of UE and BS antennas as unit vectors $\vec{p}_{UE}$ and $\vec{p}_{BS}$, respectively. As illustrated in Fig. 4(b), if a transmitted signal is observed in direction $\vec{v}$, then the polarization $\vec{p}$ of the signal is defined as projection of $\vec{p}_{UE}$ to $\vec{v}_{\perp}$ and calculated as follows: $\vec{p} = (\vec{p}_{UE} \cdot \vec{v}_{\perp}) \cdot \vec{v}_{\perp}$. It means that the observation in direction $\vec{v}$ causes additional attenuation of the reception. Here, vector $\vec{v}_{\perp}$ is perpendicular to $\vec{v}$ and parallel to a plane generated by $\vec{p}_{UE}$ and $\vec{v}$. Note, $\vec{v}$ and $\vec{v}_{\perp}$ are unit vectors.

Actually, the transducer creates a heterogeneous electric field around itself. Depending on the observed direction $\vec{v}$ relative to the transducer, the observed signal can have different polarization. The vector function of the relation between an observed direction $\vec{v}$ and the vector of the observed polarization is denoted as $\vec{F}(\vartheta, \varphi)$, where ϑ and φ are spherical coordinates of $\vec{v}$ relative to the transducer's coordinate system [11]. This means that if a signal is observed in direction $\vec{v}$ with the spherical coordinates ϑ_{dep} and φ_{dep}, the polarization of the signal is expressed as $\vec{p} = \vec{F}(\vartheta_{dep}, \varphi_{dep})$.

As illustrated in Fig. 4(a) and Fig. 3, in the case of reflection, a signal interacts with plane S_1 at point K and its polarization vector $\vec{p}$ is decomposed into the perpendicular $p_{\perp} = \vec{p} \cdot \vec{n}_2$ and parallel $p_{\parallel} = \vec{p} \cdot (\vec{n}_2 \times \overrightarrow{NLoS_{dep}})$ components relative to S_2. The decomposed components are attenuated in accordance with the Fresnel reflection coefficients $\Gamma_{\perp}$ and $\Gamma_{\parallel}$, which depend on the angle of an incident ray and the material of the surface [9]. Hence, the polarization of the reflected signal is expressed as follows:

$$\vec{p}_{ref} = \Gamma_{\perp} \cdot p_{\perp} \cdot \vec{n}_2 + \Gamma_{\parallel} \cdot p_{\parallel} \cdot \vec{n}_2 \times \overrightarrow{NLoS_{arr}}.$$

This equation shows that the reflection changes polarization of a signal, and the result of the change is inextricably linked with the value of inclination of the reflecting surface. The final attenuations caused by polarization transformations for LoS and NLoS directions can be calculated as follows:

$$G_{LoS} = \vec{p} \cdot \vec{p}_{BS},\ G_{NLoS} = \vec{p}_{ref} \cdot \vec{p}_{BS}. \tag{6}$$

C. Extension to a rough surface

In the case of a rough surface, the energy of the specularly reflected signal is reduced due to the scattering effect [12] [13]. The energy of incident signal is scattered in multiple directions instead of only the direction of specular reflection. According to the Rayleigh criterion [9], a surface is considered to be rough if the difference h between the minimum and maximum heights of a surface is higher than the critical height h_c that can be calculated as follows:

$$h_c = \frac{\lambda}{8 \cdot \cos\theta}, \tag{7}$$

where θ is the angle between the incident ray and the normal vector of a surface, as shown in Fig. 3. The attenuation coefficient ρ_s of the reflected signal caused by a rough surface is given by

$$\rho_s(\theta) = \exp\left[-8 \cdot \left(\frac{\pi \cdot \sigma_h \cdot \cos\theta}{\lambda}\right)^2\right], \tag{8}$$

where σ_h is the standard deviation of the surface's height.

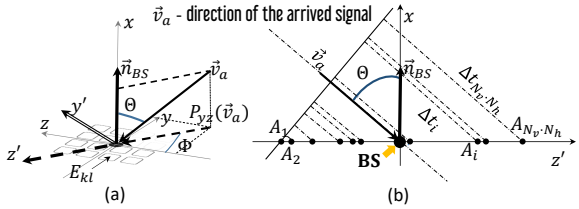

Fig. 5. (a) The geometry of an antenna array. (b) Calculation of time delays according to the receiving sequence.

IV. Simulation of MIMO antennas

In this section, we model the signal reception at the MIMO antenna side. First, we explain how to sort antenna elements according to the receiving sequence under the assumption of plane waves. Then we describe how to calculate time differences on signal reception between different antenna elements, and further extend our model to spherical waves.

As illustrated in Fig. 5(a), we assume the antenna is deployed in a plane perpendicular to O_x axis, and the normal vector of that plane is represented by $\vec{n}_{BS}$. We use $\vec{v}_a$ to denote any arrived signal ($\overrightarrow{LoS}$ or $\overrightarrow{NLoS_{arr}}$). The angle between the arrived signal $\vec{v}_a$ and $\vec{n}_{BS}$ is denoted as Θ, and the angle between axis O_z and the projection of $\vec{v}_a$ to plane O_{yz}, which is $P_{yz}(\vec{v}_a)$, is denoted as Φ. The cosines of both angles Θ and Φ can be calculated as follows:

$$\cos\Theta = -\vec{n}_{BS} \cdot \vec{v}_a,\ \cos\Phi = \frac{\vec{e}_z \cdot P_{yz}(\vec{v}_a)}{\|P_{yz}(\vec{v}_a)\|},$$

where $\vec{e}_z$ is the direction vector of the O_z axis.

A. Sorting antenna elements

The coordinates of the antenna elements are denoted as E_{kl} $(k = 1, \ldots, N_v, l = 1, \ldots, N_h)$, where N_v and N_h are the numbers of vertical and horizontal elements. As illustrated in Fig. 5(a), signal $\vec{v}_a$ first reaches the bottom right element and then all other elements sequentially. To know the sequence in which the elements receive the signal, we sort all elements according to their positions relative to the new axis $O_{z'}$, which is defined by rotating O_z with angle Φ. Hence, to sort antenna elements according to the receiving sequence, we need to rotate the old coordinate system O_{yz} counterclockwise with angle Φ to obtain the new coordinate system $O_{y'z'}$. After the rotation, coordinates in the new system can be found using the following equation:

$$\begin{pmatrix} y' \\ z' \end{pmatrix} = \begin{pmatrix} \cos\Phi & \sin\Phi \\ -\sin\Phi & \cos\Phi \end{pmatrix} \begin{pmatrix} y \\ z \end{pmatrix}. \tag{9}$$

As illustrated in Fig. 5(b), elements E_{kl} can be sorted in ascending order relative to z' coordinate, and the resulting set can be noted as $A_i, i = 1, \ldots, N_v \cdot N_h$.

B. Calculation of time differences

As illustrated in Fig. 5(b), the signal first reaches element A_1, then A_2, and etc. We use d_{12} to denote the Euclidian distance between elements A_1 and A_2 in z' coordinates. To reach element A_2 after A_1, the arrived signal spends time Δt_2,

which can be calculated as: $\Delta t_2 = \frac{d_{12} \cdot \sin\Theta}{c}$, where c is the speed of light. Hence, the time spent by the signal to reach point A_i can be calculated as: $\Delta t_i = \frac{d_{1i} \cdot \sin\Theta}{c}$, where d_{1i} is Euclidian distance between A_1 and A_i in z' coordinates.

C. Extension to spherical waves

For spherical waves [7], each element of the antenna has its own LoS and NLoS directions. Thus, the calculation of the directions should be performed separately for each element, i.e. all steps from section III should be done for each element. This approach, obviously, increases the computational complexity of the simulation, but this increase is not critical in comparison with the processing complexity of received signals.

V. Simulations

To validate our solution in terms of modeling reflections from an arbitrary surface, we implemented a simulation model in MATLAB and simulated LTE Uplink transmissions.

A. Simulation setup

The carrier's frequency F_c is set to 2.6 GHz, which is typical for LTE systems. In order to examine the channel behavior on the whole bandwidth of Uplink, we allocated the maximum bandwidth in 100 Resource Blocks (RB) to one UE, where each RB has 12 subcarriers with each having a bandwidth of 15 kHz [14]. The simulation includes one UE and one BS. The UE has only one antenna element, whereas the number of antenna elements in BS is varied from 1 to 100. Each element receives a multipath signal mixed with additive white Gaussian noise with 15 dB of SNR. The distance between elements on the antenna array is configured to be half of the wavelength $\Delta d = \lambda/2 \approx 6$ cm [10]. The BS has vertical polarization $\vec{p}_{BS}$, while the polarization $\vec{p}_{UE}$ for UE can be configured with three options: (1) Horizontal, (2) Vertical, and (3) Inclined with 45-degree polarization.

1) Environment setup: As shown in Fig. 6, we construct the environment model based on the area of the Gate of Europe in Spain obtained from Google Maps (Fig. 1). The geometrical characteristics of the buildings are obtained from the website [15]. The height of the buildings is 114 meters, and the angle of inclination is 15 degrees for both towers. In our setup, the height of BS antenna is 30 meters, and UE is 1.9 meters.

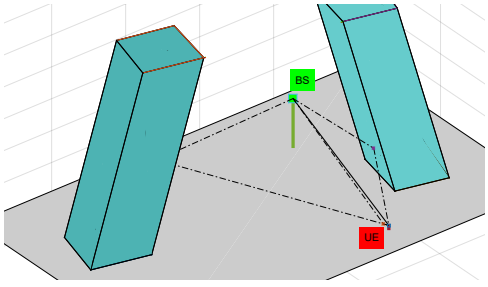

Fig. 6. The model of the Gate of Europe. Solid line is the LoS, and dashdoted lines represent reflections from inclined walls.

In order to evaluate the influence of inclined surfaces and spherical waves to channel generation, we examine both types of waves (plane and spherical) and use the following three environment setups: (1) *Inclined walls* (the real inclination of towers with 15 degrees), (2) *Vertical walls* (no inclination for the two towers), and (3) *Displaced walls* (the inclination degree is set to 1). Fig. 6 shows both the LoS path and the NLoS paths due to reflections from inclined walls.

2) The effect of wall roughness: Based on the street view from google maps, it can be seen that the most part of the surface of the buildings is covered by a glass material and the floor under the UE is made from concrete. As illustrated in Fig. 1, the gray straight elements on the surfaces make the walls rough. We assume that the gray elements stick out from the main surface with $h_{\max} = 0.2$ meters, which is higher than the critical value of the roughness h_c given in Eq. (7) for all angles of incidence θ from 0° to 86°. In our simulation, angles of reflection are smaller than 86°. Hence, the walls are considered as rough, and the attenuation coefficient given in Eq. (8) is used. From the street view, we roughly estimate the percentage of gray elements as 25% of the surface, which results in standard deviation $\sigma_h = 0.08$ m.

3) Calculation of reflection and penetration coefficients: All the physical parameters of materials and the equations used for calculating the Fresnel coefficients of reflection are used in accordance to the METIS report [7], and set as follows: (1) Glass material: relative permittivity $\varepsilon_r' = 7.0$, and conductivity $\sigma = 0.25$; (2) Concrete material: $\varepsilon_r' = 5.31$, and $\sigma = 0.0707$. The Fresnel coefficients are calculated as follows:

$$\Gamma_\perp(\theta) = \frac{\cos\theta - \sqrt{\varepsilon_r - \sin^2\theta}}{\cos\theta + \sqrt{\varepsilon_r - \sin^2\theta}}, \tag{10}$$

$$\Gamma_\parallel(\theta) = \frac{\varepsilon_r \cdot \cos\theta - \sqrt{\varepsilon_r - \sin^2\theta}}{\varepsilon_r \cdot \cos\theta + \sqrt{\varepsilon_r - \sin^2\theta}}, \tag{11}$$

where $\varepsilon_r = \varepsilon_r' - j \cdot 17.98 \cdot \sigma/f$, j is the imaginary unit, and f is the frequency in GHz. We use $f = 2.6$ in our simulation.

Our aim is to examine the reflection impact on the channel. Therefore, we assume that LoS direction and the signals reflected from the concrete floor are blocked by human. The physical parameters of a human's body are: $\varepsilon_r' = 2.97$ and $\sigma = 0.0116 \cdot f^{0.7076}$. The penetration coefficient through a human body is calculated as follows:

$$T_h = \frac{(1 - \Gamma_h^2) \cdot \exp(-j \cdot (\delta - \frac{2\pi}{\lambda} \cdot d_h))}{1 - \Gamma_h^2 \cdot \exp(-j2\delta)}, \tag{12}$$

where $\delta = \frac{2\pi}{\lambda} \cdot \sqrt{\varepsilon_r}$, d_h is the thickness of the human's body (0.6 m in our simulation), and Γ_h means Fresnel coefficient for the perpendicular and parallel components of a signal, which are calculated based on Eqs. (10) and (11), respectively. In the case of human body penetration, we assume that the antenna of UE is close enough to a human's body, i.e., $\theta = 0$.

4) Free space pathloss and attenuation coefficients: As our aim is to examine the effect of reflection, we use the following simple model of free space path loss

$$PL(d) = \frac{\lambda^2}{(4\pi d)^2}, \tag{13}$$

where d is the distance covered by a signal. The attenuation coefficients for each propagation path are calculated separately as follows based on Eqs. (6), (8), (12), (13):

- LoS path

$$K_{LoS} = G_{LoS} \cdot T_h \cdot PL(d_{LoS});$$

- NLoS path reflected from the floor

$$K_{floor} = G_{NLoS}^{concrete} \cdot T_h \cdot PL(d_{floor});$$

- NLoS paths reflected from walls

$$K_{NLoS} = \rho_s \cdot G_{NLoS}^{glass} \cdot PL(d_{NLoS}).$$

Here, $G_{NLoS}^{material}$ is the attenuation coefficient caused by polarization change in dependency to the material.

B. Simulation Results

In this section, we present the results of channel response based on LTE Uplink channel estimation procedure [16]. As the channel measurements are noisy, we average the measurements using a sliding window with length of 10 samples.

1) Scenario I (one reflecting surface): To evaluate the correctness of the simulation approach, we first run the simulation in a simple scenario with only one reflecting surface, which is the concrete floor. By intuition, it is anticipated that the power of the received signal should be higher if the antennas (UE and BS) have the same polarization and should be lower when the polarizations are perpendicular to each other. For 45 degrees of difference in polarizations, the resulting channel response should be between the two channel responses for vertical and horizontal. As illustrated in Fig. 7, this intuition is well justified: black lines represent the situation when both antennas have the same polarizations, blue lines represent the situation when the polarization of UE is inclined on 45 degrees relative to the vertical axis, and red lines represent the situation when the polarization of UE is horizontal. This indicates that, by changing the receiver's/transmitter's polarization, the connection quality can be improved. Since the UE is not located in the direction perpendicular to the antenna panel of the BS, the polarization of the transmitted signal is changing through LoS and NLoS paths. Hence, the BS can receive nonzero signals from UE when it has horizontal polarization.

In this simulation it can be observed that the more the number of antenna elements at the BS, the stronger the received signal strength, which is consistent with ideal MIMO situations. Another observation is that the discrepancy between channels generated based on plane waves and spherical waves grows with the number of antenna elements. This is caused by the fact that the maximum distance between two antenna elements increases with the increase of the number of antenna elements. When the number of elements is small, spherical waves can be accurately approximated by plane waves because the difference between these waves is minuscule. However, for an antenna with a big number of elements, the difference in receiving signal power for elements that are far away from each other is large. Hence, the approximation of spherical waves by plane waves becomes rough, which has big influences on the generation of a channel. This effect is well observed in Fig. 7: for four antenna elements, the spherical and plane channels are very close; for 16 elements the channels begin to differ and the discrepancy becomes significant for 100 elements. For example, in this particular scenario, the average difference is about 1 dB, and for other scenarios with multiple reflecting surfaces the difference could be even larger.

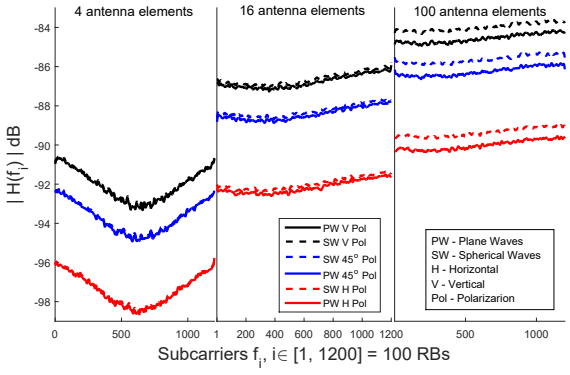

Fig. 7. Impact of polarization, different types of waves, and different number of antenna elements at BS: the polarization $\vec{p}_{UE}$ of UE has three states: V, H and 45°. The number of BS antenna elements varies between 4, 16 and 100 elements with all elements having vertical polarization.

2) Scenario II (the Gate of Europe): The main aim of this scenario is to show the importance of considering inclined surfaces in simulations. We compare channel responses in the three setups given in Section V-A1. The displaced walls are simulated to show that even a small inclination can have a significant impact on channel behavior. The polarization of BS antenna is vertical, and the UE has 45-degree polarization.

As illustrated in Fig. 8, black lines represent the model with inclined walls, blue lines represent the model with vertical walls, and the red lines represent displaced walls. Thin lines mean that channels are generated by spherical waves, and thick lines mean the channels are generated by plane waves. For the sake of simplicity, we call them as spherical channels and plane channels, respectively. As shown in Scenario I, the difference between channels generated by spherical and plane waves is small when the number of antenna elements is small. It can be seen from Fig. 8 that, for four antenna elements, the difference between spherical and plane channels is less than 0.3 dB. Moreover, all three models generate channels close to each other, and the maximum discrepancy is less than 1.4 dB. This indicates that it is feasible to use plane waves to simulate multipath channel for antennas with a small number of elements.

With the increase of the number of antenna elements, the difference between generated channels becomes significant. For 16 elements, the maximum difference between the channels with inclined walls and with vertical walls is around 8 dB. The models with vertical and displaced walls generate similar channels, and the difference between them is less than 2 dB. An interesting observation is that the spherical channel and

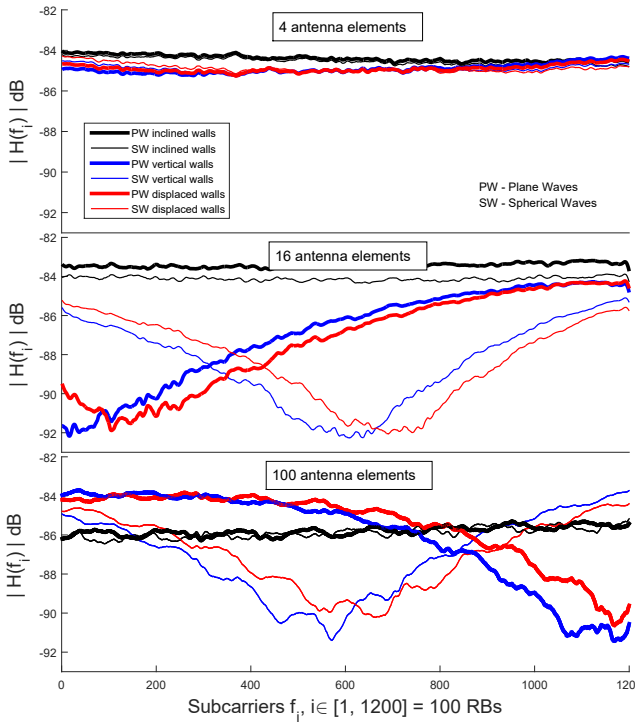

Fig. 8. Impact of number of antenna elements and different types of waves in the Gate of Europe scenario. The BS has vertical polarization, and the UE has 45° polarization. The number of antenna elements varies between 4, 16 and 100.

the plane channel are very close in the model with inclined walls, while they are significantly different in the other models. For example, the difference for inclined walls is less than 1 dB, while the difference for vertical/displaced walls is up to 6 dB. In the case of 100 elements, channels with vertical walls and displaced walls start to differ up to 3 dB, which can be vital for the LTE procedures such as signal equalization, demodulation, decoding, and etc. These results indicate that a system with large antenna arrays (e.g. massive MIMO systems) will become more sensitive to the accurate environment representation and will need very accurate channel models.

VI. Conclusion

In this paper, we demonstrated the importance of considering inclined surfaces and polarization of signals in multipath channel simulation. The simulation results indicated that inclined surfaces can have significant influence on a channel in comparison with vertical surfaces due to different propagation paths, different angles of reflection, different changes of polarizations. We further examined the difference between spherical and plane waves in terms of channel generation. We found that, for MIMO antennas with a large number of receiving elements, the difference between channels with spherical waves and plane waves is significant. In total, the obtained results indicated that the simulation of systems with massive antenna arrays should use spherical waves and take into account the spatial characteristics of wireless channels.

References

[1] A. R. Noerpel, M. J. Krain, and A. Ranade, "Measured scattered signals at 4 GHz confirm strong specular reflections off buildings," *Proc. IEEE International Conference on Communications (ICC)*, vol. 1, pp. 473–477, 1991.

[2] S. Jaeckel, L. Raschkowski, K. Börner, and L. Thiele, "QuaDRiGa: A 3-D Multi-Cell Channel Model With Time Evolution for Enabling Virtual Field Trials," *IEEE Transactions on Antennas and Propagation*, vol. 62, no. 6, pp. 3242–3256, 2014.

[3] P. Heino, "D5.3: WINNER+ final channel models," Tech. Rep., 2010.

[4] "Study on 3D channel model for LTE," Tech. Rep., 2015, 3GPP TR 36.873 V12.2.0.

[5] M. Boban, J. Barros, and O. K. Tonguz, "Geometry-Based Vehicle-to-Vehicle Channel Modeling for Large-Scale Simulation," *IEEE Transactions on Vehicular Technology*, vol. 63, no. 9, pp. 4146–4164, 2014.

[6] J. Maurer, T. Fugen, T. Schafer, and W. Wiesbeck, "A new inter-vehicle communications (IVC) channel model," *Proc. IEEE Vehicular Technology Conference, VTC2004-Fall*, vol. 1, pp. 9–13, 2004.

[7] L. Raschkowski, P. Kyösti, K. Kusume, and T. Jämsä, "METIS Channel Models," Tech. Rep., 2015.

[8] J. Heller, M. Havlena, M. Jancosek, A. Torii, and T. Pajdla, "3D reconstruction from photographs by CMP SfM web service," *Proc. 14th International Conference on Machine Vision Applications (MVA)*, pp. 30–34, 2015.

[9] O. Landron, M. Feuerstein, and T. Rappaport, "A comparison of theoretical and empirical reflection coefficients for typical exterior wall surfaces in a mobile radio environment," *IEEE Transactions on Antennas and Propagation*, vol. 44, no. 3, pp. 341–351, 1996.

[10] S. J. Orfanidis, *Electromagnetic Waves and Antennas*. Rutgers University New Brunswick, NJ, 2014.

[11] M. Narandzic, M. Kaske, C. Schneider, M. Milojevic, M. Landmann, G. Sommerkorn, and R. S. Thoma, "3D-Antenna Array Model for IST-WINNER Channel Simulations," *Proc. IEEE 65th Vehicular Technology Conference - VTC2007-Spring*, pp. 319–323, 2007.

[12] W. S. Ament, "Toward a Theory of Reflection by a Rough Surface," *Proc. IRE*, vol. 41, no. 1, pp. 142–146, 1953.

[13] P. Beckmann, "Scattering by non-Gaussian surfaces," *IEEE Transactions on Antennas and Propagation*, 1973.

[14] S. Sesia, I. Toufik, and M. Baker, *LTE - The UMTS Long Term Evolution: From Theory to Practice*. Chichester: John Wiley & Sons Ltd, 2011.

[15] [Online]. Available: www.aviewoncities.com/buildings/madrid/puertadeeuropa.htm

[16] H. Mai, Y. V. Zakharov, and A. G. Burr, "Iterative Channel Estimation Based on B-splines for Fast Flat Fading Channels," *IEEE Transactions on Wireless Communications*, vol. 6, no. 4, pp. 1224–1229, 2007.